Atmospheric Environment 46 (2012) 92–103

Contents lists available at SciVerse ScienceDirect

Atmospheric Environment

journal homepage: www.elsevier.com/locate/atmosenv

Diurnal and weekly variation of anthropogenic heat emissions in a tropical city, Singapore

Anne K.L. Quah, Matthias Roth*

Department of Geography, National University of Singapore, 1 Arts Link, Kent Ridge, Singapore 117570, Singapore

ARTICLE INFO

Article history:
Received 17 July 2011
Received in revised form
6 October 2011
Accepted 7 October 2011

Keywords:
Anthropogenic heat
Waste heat
Energy use
Tropical urban climate
Singapore

ABSTRACT

The present study estimates the temporal variability of the anthropogenic heat flux density (Q_F) for three common land use types found in Singapore between October 2008 and March 2009. Q_F is estimated by separately considering the major sources of waste heat in urban environments, which are heat release from vehicular traffic, buildings and human metabolism, respectively. The individual components of Q_F are calculated by using a combination of top-down and bottom-up modelling approaches of energy consumption applied to the local context. Results show that over a 24-h period, magnitudes of mean hourly Q_F reach maximum values of 113 W m^{-2} in the commercial, 17 W m^{-2} in the high-density public housing and 13 W m^{-2} in the low-density residential areas, respectively. Buildings are found to be the major source of anthropogenic heat (primarily related to space cooling) in each study area, contributing to between 49–82% of Q_F on weekdays and 46–81% on weekends. The spatial and temporal variations of Q_F are attributed to differences in traffic volume, building energy consumption and population density. This is one of the first anthropogenic heat studies carried out in a tropical city and the results show that Q_F can be substantial and of the same order of magnitude as calculated for city centres in mid-latitude cities during winter time.

1. Introduction

Cities cover only about 2% of the global land area, yet they are responsible for ~70% of the world's energy consumption (International Energy Agency, 2008a). Energy demand by urban dwellers and activities associated with running a city are predicted to increase over the next 20 years and probably beyond (e.g. International Energy Agency, 2009). The consumption of energy for human activities produces waste heat, water vapour and pollutants, thereby directly affecting the temperature, humidity, air quality and human health in the urban environment. Heat and moisture emissions associated with energy consumption in cities has been largely ignored or overly simplified in many studies of the urban climate (Sailor, 2011). This is particularly true for cities located in tropical climate, where understanding of the physical processes operating in the urban atmosphere in general is still rudimentary (Roth, 2007).

In order to effectively address the climate-related environmental issues that urban areas face as a consequence of their energy consumption patterns, it is essential to first have a better understanding of the nature of their physical climatology. Fundamental to this understanding is the building-air volume formulation of the urban (surface) energy balance (UEB) which is expressed as (Oke, 1987):

$$Q^* + Q_F = Q_H + Q_E + \Delta Q_S + \Delta Q_A \quad \left[\mathrm{W\,m^{-2}}\right] \tag{1}$$

where Q^* is the net all-wave radiation flux, Q_H and Q_E are the turbulent sensible and latent heat fluxes, respectively, ΔQ_S is the net heat storage flux and ΔQ_A the net horizontal advective heat flux. Q_F is the anthropogenic heat flux and focus of the present study. Positive values on the left-hand side of Eq. (1) are inputs to the system, while positive values on the right-hand side are outputs or losses.

The majority of UEB studies which in the past have been carried out primarily in temperate (e.g. Grimmond and Oke, 1999; Spronken-Smith, 2002) and in fewer cases tropical (e.g. Roth, 2007) cities, neglect the Q_F term, which is essentially the energy released from human sources such as vehicles, commercial and residential buildings, industry, power plants and human metabolism. Disregard for Q_F stems primarily from its modest magnitude relative to the other fluxes in Eq. (1) and also from difficulties in assessing the magnitude of this particular term (e.g. Garcia-Cueto et al., 2003; Spronken-Smith et al., 2006; Sailor, 2011). Nevertheless, the interest in quantifying Q_F

* Corresponding author. Tel.: +65 6516 6103; fax: +65 6777 3091.
E-mail address: geomr@nus.edu.sg (M. Roth).

1352-2310/$ – see front matter © 2011 Elsevier Ltd. All rights reserved.
doi:10.1016/j.atmosenv.2011.10.015

has been growing over the last few years, especially for densely populated mid-latitude cities such as Tokyo, Seoul and London. This trend is perhaps the result of an increased awareness of the findings of past Q_F studies, which have shown that for densely populated cities with high energy demands, Q_F can potentially be an important or even dominant component of the UEB with the potential to influence urban climates. For example, Grimmond (1992) observed that more than 10% of the winter-time energy input ($Q^* + Q_F$) in Vancouver was accounted for by Q_F, while Ichinose et al. (1999) estimated Q_F in central Tokyo to reach 908 W m^{-2} in the daytime during summer months and as much as 1590 W m^{-2} during the early morning hours in winter. Temperature simulations by Fan and Sailor (2005) suggested that in winter, Q_F contributes about 2–3 °C to the nighttime urban heat island (UHI) of Philadelphia. In addition, numerical simulations by Chen et al. (2009) concluded that Q_F contributes 43.6% (54.5) in summer (winter) to the UHI intensity in Hangzhou City. The same study also concluded that waste heat emissions via Q_F strengthen the UHI circulation and improve near-surface turbulent activity, with stronger effects observed at night than during daytime (Chen et al., 2009).

The magnitude of Q_F varies greatly not only between cities but also within cities depending on per capita energy use, population density, meteorological conditions and background climate. According to Oke (1988) the mean annual magnitude of Q_F for large cities ranges from 20 to 160 W m^{-2}. For US cities, values between 20 and 40 W m^{-2} in summer and 70–210 W m^{-2} in winter have been reported (Taha, 1997). An updated summary of Q_F estimates from mostly mid-latitude cities located in the northern hemisphere shows higher winter (cold season) values compared to those estimated for the summer (where data exists), and extreme peak values under certain conditions (e.g. winter time and/or in densely built areas) when Q_F can exceed the net radiation input into the system (Table 1).

Most studies estimate Q_F using either the inventory-based or energy balance closure approach. Estimating Q_F based on the former is the classical and most frequently used approach (e.g. Grimmond, 1992; Klysik, 1996; Sailor and Lu, 2004; Pigeon et al., 2007; Smith et al., 2009). Its earliest application is likely that by Torrance and Shum (1975) who estimated the mean annual Q_F of an unspecified densely populated city as 83.7 W m^{-2}. The inventory-based method can be further divided into top-down and bottom-up approaches using utility scale consumption data or data obtained from energy consumption surveys, respectively. The former requires data at large aggregate scales (e.g. yearly) for the purpose of downscaling to smaller scales of interest (e.g. hourly) whereas the latter uses energy consumption estimated at small-scales (e.g. individual buildings) in order to scale the information up to larger scales of interest (e.g. city-scale). The theoretically simpler and more straightforward energy balance closure approach calculates Q_F as a residual term of the UEB (Eq. (1)). However, it has the inherent problem of accumulating errors arising during the measurement of Q_H and Q_E and modelling of ΔQ_S and ΔQ_A (which cannot be directly measured) in the residual Q_F. Therefore, only few studies have used the energy balance closure method to estimate Q_F (e.g. Offerle et al., 2005; Pigeon et al., 2007).

Data from a range of cities is necessary to arrive at a more comprehensive understanding of the effects of anthropogenic heat emission and their effects on the urban thermal environment and other attributes of the urban climate system. Most available studies have been conducted primarily in mid-latitude regions with the exception of Hong Kong, Mexico City and São Paulo (Table 1). The objective of the present study is therefore to estimate the anthropogenic heat emissions in Singapore which is a fast-growing metropolis located in a tropical climate. The specific goals are to:

i. Estimate the diurnal and weekly variations of Q_F in this tropical city where the magnitude of Q_F can potentially be quite large owing to strong demand for air-conditioning throughout the year;
ii. Analyse the results with respect to land use types and energy consumption patterns; and
iii. Provide an assessment of the potential impact of Q_F on the urban climate of Singapore.

2. Description of study area

Singapore (1°09′N to 1°29′N, 103°36′E to 104°25′E) is an island city-state located at the southern tip of the Malay Peninsula. Due to its maritime position and proximity to the equator (~130 km to its north) Singapore experiences a typical equatorial wet tropical climate with uniformly high temperatures (mean monthly temperatures range from 26.4 to 28.3 °C) and abundant rainfall (mean annual average ~2192 mm) throughout the year (National Environment Agency, 2009). The most significant annual climate variation is caused by the seasonal reversal of wind directions resulting in two distinctive monsoon seasons. Moderately strong surface winds from the northeast characterise the slightly cooler winter months (December–March) whereas weaker southwest winds dominate during the warmer summer months (May–September). During the inter-monsoon seasons, wind direction is highly variable and mean wind speeds are generally low. Peak rainfall occurs between November and January, caused by storms associated with the northeast monsoon. On the other hand, slightly lower than average precipitation is measured during the southwest monsoon season. Synoptic scale climatic variations are absent as a result of the country's small size and lack of pronounced topographical features (Singapore's highest natural point is only 164 m above sea-level).

Much of Singapore is built-up with residential buildings, industrial estates and commercial/business structures in an often fragmented fashion. 10% of Singapore's land is committed as green space (half of which are nature reserves), but together with extensive roadside greenery and an island-wide Park Connector Network, some statistics declare that close to half of the country is covered by vegetation in 2007 (Ministry of the Environment and Water Resources, 2009). With a population of >5 million in 2011, average population density exceeds 7000 persons km^{-2}. For the purpose of the present study, one area each was selected from Singapore's commercial, high-density public housing and low-density residential land uses, respectively. These locations represent some of the more common land use types found in Singapore. The three selections are further important because public housing estates house ~82% of the population and the largest anthropogenic heat fluxes are expected in commercial areas. It also proved to be less difficult to obtain the necessary data to carry out the present study in these areas compared to other land use types (e.g. industrial estates). Similar to previous studies (e.g. Grimmond, 1992; Pigeon et al., 2007) the final study area included the region within a 500 m circle centred on a landmark for each selected land use type. Ideally, the land use of each study area should be fully homogeneous, i.e. being used for the same type of activity such as commercial or residential, in order to obtain Q_F estimates that are fully representative of the particular land use. However, Singapore's urban layout makes it extremely difficult, if not impossible, to identify fully homogeneous built-up areas in terms of land use. While the land use of each study area may not be homogeneous, its predominant activity corresponds to the type of land use which it represents.

The study area representing the commercial land use (COM) is characterised by mainly commercial buildings, shopping malls, hotels and office blocks (heights of up to 218 m and plot ratio

Table 1
Chronological summary of mean anthropogenic heat flux density (Q_F) for different cities.

Year	City, Country	Latitude	Population density[a] (persons km^{-2})	Annual average Q^* (W m^{-2})	Q_F (W m^{-2})			Approach used to determine Q_F[b]	Reference
					Annual	Summer	Winter		
1952	Sheffield, England	54°N	10,420	56	19	–	–	B	Garnett and Bach (1965)
1961	Montreal, Canada	45°N	14,102	52	99	57	153	B	Summers (1965) cited in Kalma and Byrne (1975)
1963	Cincinnati, US	39°N	2500	–	26	–	–	B	Bach (1970)
1965	New York City, US	40°N	10,550	–	47	–	–	B	Department of Health, Education and Welfare (1967)
1965–70	Hamburg, Germany	53°N	2450	–	13	–	–	B	Harleman (1971)
1965–70	Los Angeles, US	34°N	2000	108	21	–	–	B	Harleman (1971)
1967	Manhattan, US	40°N	28,810	93	159	53	26	B	Bornstein (1968)
1967	West Berlin, Germany	52°N	9830	57	21	–	–	B	SMIC (1971)
1967–75	Fairbanks, US	64°N	550	18	6	–	–	B	Harleman (1971)
1970	Budapest, Hungary	47°N	11,500	46	43	32	51	B	Probald (1972)
1970	Moscow, Russia	56°N	7300	42	127	–	–	B	SMIC 1971)
1970	Munich, Germany	48°N	3000	–	9	–	–	B	Geiger, B (1974) cited in Kalma and Byrne (1975)
1970	Vancouver, Canada	49°N	5360	57	19	15	23	B	Yap and Oke (1974)
1970–74	Osaka, Japan	35°N	14,600	–	26	–	–	B	Ojima and Moriyama (1982)
1971	Hong Kong, China	22°N	37,200	≈110	33	41	32	B	Newcombe (1976)
1971	Sydney, Australia	34°S	690	–	2	–	–	B	Kalma et al. (1972)
1973	Brussels, Belgium	50°N	8020	–	28	–	–	B	Kalma and Byrne (1975)
1984–86	Lodz, Poland	51°N	10,600	–	29	12	54	B	Klysik (1996)
	Densest area		–	–	34	14	73	B	
	Suburb		–	–	4		8	B	
1986	Jerusalem, Israel	32°N		–	11	–	–	B	Swaid (1993)
1986–94	Tokyo, Japan	35°N	–	–	–	284[c]	–	B	Moriwaki et al. (2008)
1987	Vancouver, Canada	49°N	–	–	–	–	~11	B	Grimmond (1992)
1989	Tokyo, Japan	35°N	–	–	–	908[c]	1,590[c]	B	Ichinose et al. (1999)
1991–92	Reykjavik, Iceland	64°N	2684	–	35	–	–	B	Steinecke (1999)
1993–98	Mexico City, Mexico	19°N	–	–	20	–	–	B	Tejeda and Jauregui (2005)
2000	Various US cities[d]	37–40°N	–	–	–	30–60	70–75	B, T	Sailor and Lu (2004)
2001–02	Basel, Switzerland	47°N	–	–	–	–	–	Energy balance	Christen and Vogt (2004)
	City centre		–	–	20	–	–		
	Suburb		–	–	5	–	–		
2001–02	Lodz, Poland	51°N	–	–	–	−3	32	Energy balance	Offerle et al. (2005)
2002	Philadelphia, US	39°N	–	–		60	9		Fan and Sailor (2005)
2002	Gyeonggi, South Korea	37°N	1000	–	28	–	–	T	Lee et al. (2009)
2002	Incheon, South Korea	37°N	2700	–	53	–	–	T	Lee et al. (2009)
2002	Seoul, South Korea	37°N	17,000	–	55	5–10	35–75	T	Lee et al. (2009)
2004–05	Toulouse, France	43°N	–	–	–	–	–	B, Energy balance	Pigeon et al. (2007)
	City centre		–	–	–	25	100		
	Suburb		–	–	–	<5	5–25		
2004–07	São Paulo, Brazil	23°N	–	–	–	20.1[c]	20.3[c]	T	Ferreira et al. (2011)
2008	Manchester, England	53°N	3779	–	11	–	–	B	Smith et al. (2009)
2008–09	Singapore	1°N	–	–	–	–	–	B, T	Present study
	Commercial		3,000[e]	–	85[f]	–	–		
	Residential (high-density)		21,000[e]–	–	13[f]	–	–		
	Residential (low-density)		7,000[e]	97	11[f]	–	–		

[a] Values refer to population density of the entire city, excluding Singapore.
[b] B – Inventory-based bottom-up modelling approach; T – Inventory-based top-down modelling approach.
[c] Represents maximum mean hourly value.
[d] Chicago, San Francisco and Philadelphia.
[e] Resident population density within the area of interest.
[f] Represents mean hourly value. It is listed under the 'Annual' column as Singapore does not have a distinct summer and winter season.

between 2.8 and 5.6) (Fig. 1a). It is part of a larger area (Orchard Road District) which experiences the city's highest level of commercial activity and is also the location of the highest observed UHI magnitude (Chow and Roth, 2006). The high-density public housing land use comprises primarily of high-rise government-built Housing and Development Board (HDB) flats (average height ~39 m; plot ratio 2.8–3.5) and is represented by a study area located in the Clementi precinct (Fig. 1b). These HDB flats are a highly visible feature of Singapore's built environment. The third study area was selected to represent the low-density residential land use in Singapore (RES). Private houses and apartment buildings (average height ~9 m; plot ratio 1.4–3.0) are the predominant urban features of RES (Fig. 1c). Overall, the selection of these three specific study areas will allow for comparisons to be made between areas of different activities, population densities and traffic volumes to aid in the understanding of the nature of Q_F across different land uses in Singapore.

3. Conceptual framework used to estimate Q_F

Q_F was estimated as the sum of the major sources of waste heat (e.g. Sailor and Lu, 2004):

$$Q_F = Q_V + Q_B + Q_M \quad \left[\mathrm{W\,m^{-2}}\right] \tag{2}$$

where Q_V, Q_B and Q_M are the contributions to the anthropogenic heat flux from traffic, buildings and human metabolism, respectively. The three terms on the right-hand side of Eq. (2) were

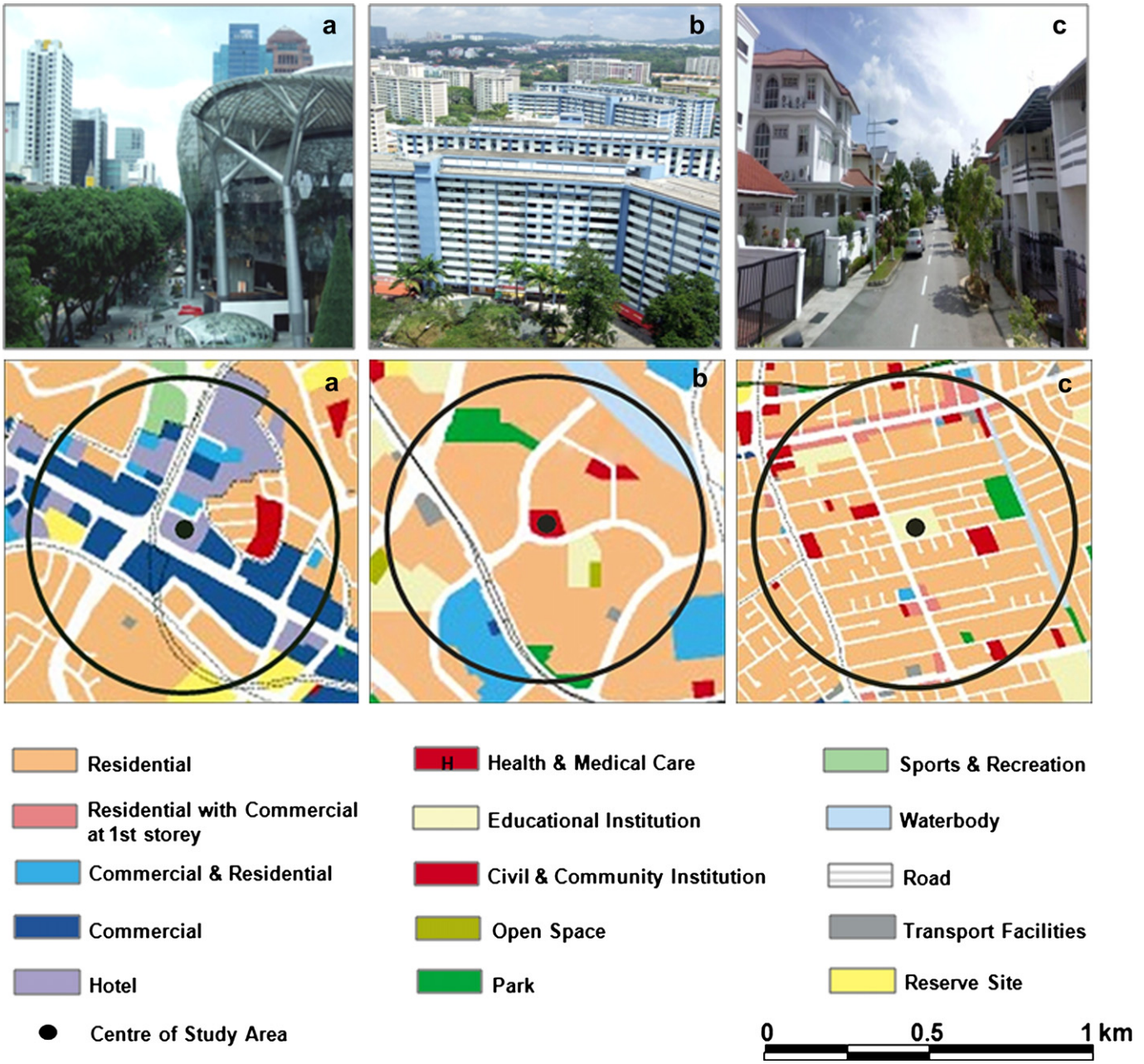

Fig. 1. Photographs and detailed land use of the three study areas which are demarcated by black circles of 500 m radius. (a) commercial (COM), (b) high-density public housing (HDB) and (c) low-density residential (RES). The colour coding for 'Residential' does not differentiate between high-density and low-density residential areas. Source: Urban Redevelopment Authority, 2008.

determined using different inventory-based modelling approaches, viz. bottom-up for Q_V and Q_B and top-down for Q_M.

Although the bottom-up modelling approach is generally more accurate than the top-down approach (Sailor, 2011), a combination of these two approaches was adopted in the present study due to issues associated with data availability, which is a challenge in most Q_F studies. The inventory-based approach also assumes that energy consumption equals anthropogenic heat emissions. This assumption ignores the fact that energy used in the urban context is also embodied in the other components of the UEB and is partially emitted as Q_H and Q_E, which further has the potential to modify the long-wave radiation budget of the urban surface. Given that there are currently no viable alternative solutions to address this issue if Q_F is to be estimated using the inventory-based method, the present study uses the same approach as applied by the majority of past studies (e.g. Grimmond, 1992; Ichinose et al., 1999; Sailor and Lu, 2004; Pigeon et al., 2007). The following sections detail the application of the modelling framework to the present study areas for a six-month period between October 2008 and March 2009. This period, although slightly cooler and wetter than the summer months, is representative of general conditions given the absence of a pronounced seasonality in the climate which would primarily affect building-related emissions. In the present case, these emissions are largely related to energy use for

air-conditioning given the uniformly high day and nighttime temperatures.

3.1. Anthropogenic heat emissions from traffic

Only vehicular traffic is considered in the present study because direct emissions from other transport means such as trains are small (absent in the case of RES, only one below and above ground subway in COM and HDB, respectively). Hourly heat emission from the combustion of vehicle fuels, $Q_V(h)$, was computed according to Grimmond (1992):

$$Q_V(h) = \left[\sum_{ijk}\left(n_{vijk}(h) \times EV_{ij} \times d_k\right)\Big/3600\right]\Big/A \ \left[\mathrm{W\,m^{-2}}\right] \quad (3)$$

$$EV_{ij} = \left(NHC_j \times \rho_j\right)\Big/FE_{ij} \ \left[\mathrm{J\,m^{-1}}\right] \quad (4)$$

where h is local time (hour; solar time + 1 h), subscripts i, j and k indicate vehicle class, fuel type and road segment, respectively, $n_{vijk}(h)$ is the hourly total number of class i vehicles consuming fuel type j and travelling on road segment k at hour h, d_k is vehicle distance travelled on road segment k (m), EV_{ij} is the energy used per vehicle of class i consuming fuel type j (J m^{-1}), A is the size of the study area (m^2), NHC_j is the net heat combustion of fuel type j (J kg^{-1}), $\tilde{n}_j$ is the density of fuel type j (kg l^{-1}) and FE_{ij} is the mean fuel economy of class i vehicles consuming fuel type j (m l^{-1}). Eq. (3) indicates that Q_V is a function of the number of vehicles, energy used by vehicles, and distance travelled by vehicles within the study area.

3.1.1. Estimation of vehicle numbers

The hourly number of vehicles on each road segment in each of the three study areas was obtained from the Singapore Land Transport Authority (LTA). The total number of vehicles travelling along each road segment was further broken down into nine vehicle classes because different vehicle types consume different amounts of energy: Cars $\leq$ 1600 cc (36%), cars $>$ 1600 cc (25%), motorcycles and scooters (17%), light goods vehicles (11%), heavy goods vehicles (4%), taxis (3%), buses (2%), very heavy vehicles (1%) and goods-cum-passenger vehicles (1%). This information was then used together with hourly traffic count data corresponding to the road segments of interest to estimate the number of vehicles per vehicle class on every road segment identified within COM, HDB and RES.

Two assumptions were made in using above method. First, at any hour of the day vehicles of all classes were present on all road segments in the study areas. Second, the distribution of vehicle classes on each road segment of interest remained the same throughout the day. Both assumptions are probably not fully reflective of reality. However, without actual data of the hourly distribution of vehicle classes, these assumptions were necessary to produce the hourly data for the present study. Spot verification in the field showed that vehicles belonging to all classes were found in each study area in accordance with the distribution mentioned above.

3.1.2. Estimation of energy used and distance travelled by vehicles

Energy usage varies among vehicle classes due to differences in fuel type used and fuel economy. In the present study every vehicle was assumed to be powered by either unleaded petrol or diesel given that only a very small percentage (0.06%) of all vehicles in Singapore run on other fuel types, such as compressed natural gas (LTA, 2008). Tables 2 and 3 summarise the net heat combustion and fuel density values of unleaded petrol and diesel, and the mean fuel economy values representative of each vehicle class considered. The value representative of the energy used per vehicle for each vehicle class was calculated by substituting the values of net heat combustion, fuel density and fuel economy into Eq. (4) and is also included in Table 3. The present energy usage values are 3–14% lower compared to those used by Pigeon et al. (2007). Calculating representative energy usage values for different vehicle classes offers an improved estimate of Q_V over studies which use only one value thought to be representative of the entire vehicle fleet (e.g. Sailor and Lu, 2004).

Traffic count data is available from LTA for vehicles travelling along particular road segments, defined as the stretch of road between two traffic junctions. Vehicles are assumed to have travelled the entire length of a particular segment which was obtained by digitising every road segment within each study area (Fig. 1) and calculating its length in a Geographic Information System (GIS).

3.2. Anthropogenic heat emissions from buildings

The energy consumed within buildings is typically used for heating, cooling, ventilation, lighting and operating appliances. Despite an actual time lag between energy consumption and heat emissions into the atmosphere, the present study assumed that all energy consumed within buildings was instantaneously rejected into the atmosphere as sensible waste heat. The assumption was made due to uncertainties in specifying this time lag which is dependent on a complex combination of various factors, such as building design, ventilation, insulation and the type of HVAC (Heating, Ventilation and Air-conditioning) system used.

Electricity and gas are the two types of energy currently consumed by commercial and residential buildings in Singapore. However, only electricity contributions to Q_B were considered in the present study as the consumption of gas is relatively minimal, contributing only 3% of Singapore's total annual energy consumption compared to that of electricity in Singapore's commercial and residential sectors (International Energy Agency, 2008b). An equation proposed by Grimmond (1992) was modified and applied to estimate hourly Q_B values:

$$Q_B(h) = \sum_k E_k(h)/A \ \left[\mathrm{W\,m^{-2}}\right] \quad (5)$$

where subscript k indicates building number (each building considered was assigned a building identification number) and $E_k(h)$ is the mean hourly electricity consumption of building k at hour h (W).

Because electricity consumption for buildings was only available at daily and sometimes even coarser scales (i.e. monthly or yearly), $E_k(h)$ was estimated by mapping the building's electricity consumption data to its representative electricity load profiles (similar to Sailor and Lu, 2004). These profiles were developed at the monthly, weekly, daily and hourly scales using data from

Table 2
Net heat combustion and fuel density of unleaded petrol and diesel.

Fuel type	Net heat combustion ($\times 10^6$ J kg^{-1})	Fuel density range[a] (kg l^{-1})
Unleaded Petrol	46.4	0.74–0.76 (0.75)
Diesel	42.8	0.83–0.86 (0.85)

[a] Fuel density varies with ambient temperature; as such the mid-point value (in parenthesis) was used. Source: Shell Eastern Petroleum (Pte) Ltd (personal communication, 2008).

Table 3
Mean fuel economy and representative values of energy used per vehicle, according to the different vehicle classes in Singapore.

Vehicle class	Mean fuel economy ($m\ l^{-1}$)	Energy used per vehicle ($J\ m^{-1}$)
Motorcycles and scooters	29,411.76	1183.2
Goods-cum-passenger vehicles[a]	13,333.33	2728.5
Cars (≤1600 cc)	10,416.67	3340.8
Light goods vehicles[a]	9900.99	3674.4
Goods-cum-passenger vehicles[b]	9345.79	3723.6
Taxis	9090.91	4001.8
Cars (>1600 cc)	8264.46	4210.8
Light goods vehicles[b]	7092.20	4906.8
Heavy goods vehicles	6849.32	5311.5
Buses	2178.65	16,698.4
Very heavy goods vehicles	1980.20	18,371.9

[a] Diesel-powered engines.
[b] Petrol-powered engines. Sources: Land Transport Authority (personal communication, 2008); Volkswagen (2008).

various building energy audit reports and a pilot study on household electricity consumption in Singapore (PREMAS Energy Centre, 2004). Every building identified within COM, HDB and RES was categorised into one of the eight building categories for which representative electricity load profiles were readily available (commercial, residential, hotel, educational institution, health and medical care, community institution, transport facility and mixed development) (Fig. 2). While the top-down approach was used to estimate the hourly electricity consumption of individual buildings, E_k (h), a bottom-up approach was used to determine the total electricity consumption within each study area.

3.3. Anthropogenic heat emissions from human metabolism

The approach used to estimate Q_M followed Grimmond (1992). Each day was divided into two periods, 'active' and 'sleep', defined as 07:00–22:59 h and 23:00–06:59 h, respectively. Q_M was calculated using:

$$Q_M(h) = \sum [M_p \times n_p(h)]/A \quad \left[\mathrm{W\ m^{-2}}\right] \tag{6}$$

where subscript p represents the time period ('active' or 'sleep'), M_p is the metabolic heat produced per person during time period p ($\mathrm{W\ person^{-1}}$) and n_p refers to the total number of people within the study area during time period p.

3.3.1. Calculation of metabolic heat production values

The metabolic heat produced from activities most commonly carried out in the study areas was calculated using data from Fanger (1972) (Table 4). In the absence of population data engaging in these different activities over the course of a day, the total

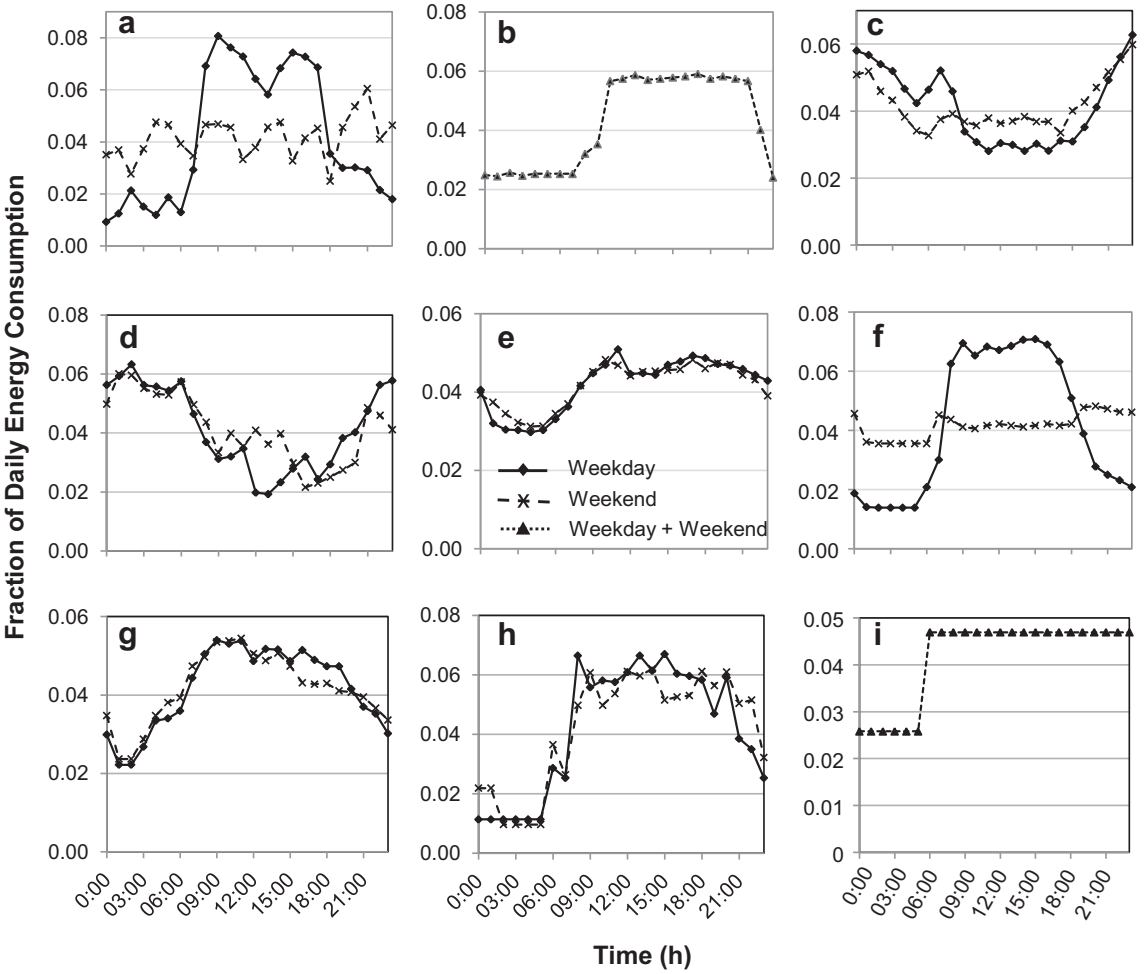

Fig. 2. Representative hourly electricity load profiles of various building types, expressed as a fraction of total electricity consumed over 1 day. Sources: (a) Ministry of Education (2002); (b) Plaza Singapura (2006); (c and d) Energy Market Authority, personal communication (2009); (e) Shangri-La Hotel Singapore (2002); (f) National Institute of Education (2003); (g) Tan Tock Seng Hospital (2004); (h) The American Club Singapore (2004); (i) Thong et al. (2005).

Table 4
Metabolic heat production values of activity types most commonly carried out in COM, HDB and RES.

Activity	Approximate metabolic heat production	
	W m^{-2}	W[a]
Sleeping	41	69
Office work (typing, filing, etc)	52–70	88–119 (104)[b]
Driving	58–100	99–197 (148)[b]
Shopping	93	158
Domestic work (cleaning, cooking)	93–198	158–336 (247)[b]
Walking (level ground, 3.2 km h^{-1})	116	198

[a] Calculated based on an adult human body surface area of 1.7 m^2.
[b] Average value given in parenthesis were used in the calculations. Source: Fanger (1972).

metabolic heat produced during the 'active' period was estimated as 171 W (average of metabolic rates of daytime activities: office work, driving, shopping, domestic work and walking), whereas for the 'sleep' period 69 W was used (Table 4).

3.3.2. Estimation of hourly population

Since the breakdown of actual resident and daytime population in the study areas was unavailable, traditional census data was interpolated to estimate the resident population. Additional sources such as working population and shopper data were obtained to improve the estimates of the daytime population. The population in the three study areas during the 'active' period was considered to be equivalent to their daytime population (i.e. non-working resident population; for COM shopper, worker and pedestrian populations were also included) while that for the 'sleep' period was assumed to be the same as their resident population (for COM hotel guests were also included) (Table 5).

The considerable population increase observed in COM during the weekday and weekend 'active' periods relative to the 'sleep' periods is due to the influx of workers and shoppers into this area. The population consequently decreased in HDB and RES during the 'active' period (when most people are in the city centre for work or shopping), and a population increase is observed during the 'sleep' period (when most people return home from the city centre).

4. Results

4.1. Diurnal variation of anthropogenic heat emissions from vehicles, buildings and human metabolism

Ensemble averages of the diurnal variation of Q_V for all 181 days of the observation period are shown in Fig. 3. Q_V was largest at COM

Table 5
Estimated weekday and weekend population of COM, HDB and RES at any hour of the 'sleep' (23:00 h–06:59 h) and 'active' (07:00 h–22:59 h) periods.

Study area	Estimated hourly population		
	'Sleep' period (weekdays and weekends)	'Active' period (weekday[a])	'Active' period (weekend[b])
COM	9846[c]	29,802[d]	41,275[e]
HDB	16,656	8316	16,656
RES	5770	3359	5770

[a] Monday to Friday.
[b] Saturday, Sunday and Public Holidays.
[c] Comprises 2595 residents and 7251 hotel and serviced apartment guests.
[d] Comprises non-working residents (1449), shoppers (13,389), workers (13,448) and pedestrians (1476).
[e] Comprises non-working residents (2595), shoppers (25,010), workers (9924) and pedestrians (3746).

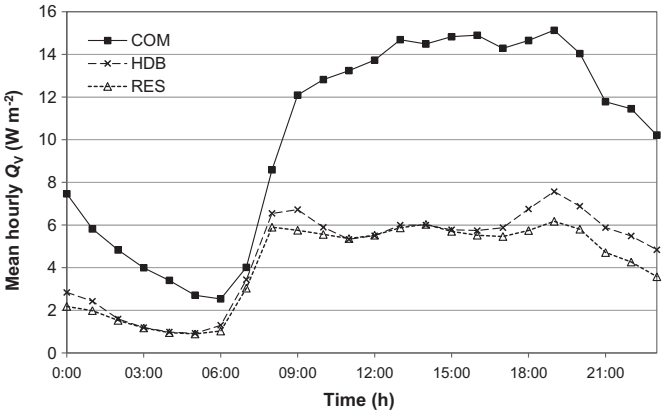

Fig. 3. Ensemble average from 181 days of diurnal variation of Q_V at COM, HDB and RES.

at every hour of the day with a maximum value of 15 W m^{-2} recorded at 19:00 h. Peak diurnal Q_V values at HDB (8 W m^{-2}) and RES (6 W m^{-2}) were also observed at 19:00 h with secondary, slightly smaller peaks at 08:00 h. As expected, peak emissions correspond to the morning and evening rush hours. The systematically larger values in COM reflect the much heavier traffic found in the commercial centre.

The corresponding diurnal variation of Q_B is presented in Fig. 4. Estimates for COM were significantly larger compared to those for HDB and RES at every hour of the day. The high mean hourly Q_B values observed from 08:00–22:00 h at COM arise from the high level of electricity consumed by offices, shopping malls and hotels, mainly for air-conditioning and to a lesser extent lighting purposes during this period. In comparison, HDB and RES comprise mainly of residential buildings which consume substantially lower amounts of electricity relative to the non-residential buildings which dominate COM. In addition, the total built-up area and built-density of COM is larger than for HDB and RES. Hence, more electricity is needed to meet the cooling/ventilation needs of the former compared to the two residential sites. Besides magnitude there are also differences in the diurnal variation between the commercial and residential sites. The former has its highest values during daytime, extending into the late evening when commercial activity starts to cease (shops close around 21:00–22:00 h). On the contrary, values start to increase in the two residential sites in the evening with a peak at 23:00 h when people return home and use electricity for e.g. lighting, running audio-visual and computer

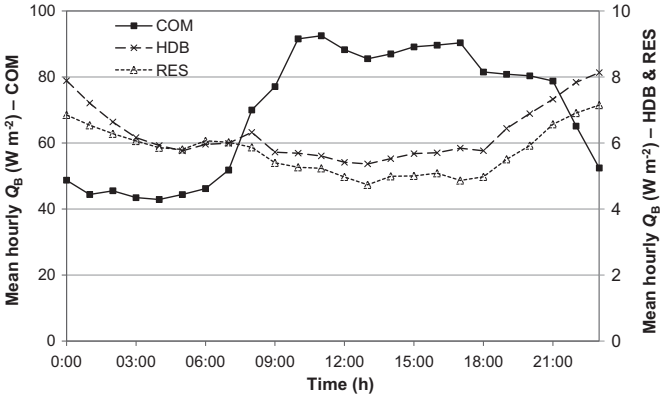

Fig. 4. Same as Fig. 3 but for Q_B.

equipment and cooling their residential spaces in the early hours of the night.

The diurnal building energy use profile of COM is similar to the winter time total diurnal energy use profile of offices, commercial buildings and hotels in Tokyo (Moriwaki et al., 2008), albeit less pronounced. The diurnal building energy use profiles of HDB and RES are somewhat different from the summer and winter-time energy use profiles of domestic buildings in mid-latitude cities such as the Greater Manchester region (Smith et al., 2009). Energy usage levels in the latter peak about 4 h earlier (around 19:00 h during summer and winter) than observed in the residential areas of the present study because air-conditioning, which constitutes the bulk of energy consumed in households, is generally switched on late in the evening.

The diurnal variation of mean hourly Q_M is shown in Fig. 5, and reflects clear daytime *vs*. nighttime activity differences. During the 'active' period (i.e. 07:00–22:59 h), COM had the highest value of 7 W m^{-2} whereas the lowest value of 0.9 W m^{-2} was calculated for RES. A slightly different observation was made for the 'sleep' period (i.e. 23:00–06:59 h) during which the highest value (1.5 W m^{-2}) was estimated at HDB and the lowest value (0.5 W m^{-2}) at RES. As expected, magnitudes of Q_M were always larger during the 'active' period compared to the 'sleep' period by a factor of 2 (HDB and RES) and 8 (COM), respectively. In the case of COM, this observation results from a larger (3–4 times) 'active' compared to the 'sleep' period population (Table 5). However, to explain the diurnal variation of mean hourly Q_M at HDB and RES, population size has to be considered together with the types of activity engaged in. Although the estimated 'active' period population in the residential areas were either lower (for weekdays) or equal (for weekends) compared to their 'sleep' period population throughout the week (Table 5), the amount of metabolic heat produced by a person engaging in daytime activities (e.g. domestic chores, shopping and office work) is about 3 times higher than that for nighttime activities which was assumed to consist only of sleeping. Thus, lower population counts but higher metabolic rates during the 'active' period compared to the 'sleep' period result in the larger Q_M magnitudes observed at HDB and RES during the 'active' period for every day of the week.

4.2. Total anthropogenic heat flux

The diurnal variation of mean hourly Q_F and its individual components is shown in Fig. 6. The highest values were calculated for COM reaching 113 W m^{-2} at around 11:00 h. Maximum values at HDB (17 W m^{-2}) and RES (13 W m^{-2}) were observed at about 19:00 h and 20:00 h, respectively. Minimum values of 7 W m^{-2} were recorded at RES at around 05:00 h. The diurnal Q_F profile of COM is dominated by the magnitude and shape of building energy-related emissions resulting in the largest Q_F values occurring during the daytime and evening. Q_B was also a major component of Q_F at the two residential sites with Q_V being of comparable size during the daytime. However, unlike in COM, the shape of the diurnal HDB and RES Q_F profiles is dominated by traffic-related peak emissions, and displays maximum values at 08:00 h and 19:00 h, respectively. All three study areas show minimum values at about 05:00 h.

Fig. 7 shows the average weekday and weekend Q_F diurnal profiles. For both periods the values were always largest at COM, averaging about 86 W m^{-2} on weekdays and 82 W m^{-2} on weekends, with minimal differences in their diurnal variation. The reverse was observed for HDB and RES. The values for HDB averaged 14.0 (15.0) W m^{-2} on weekdays (weekends) and 11.2 (11.4) W m^{-2} for RES, respectively. At each study area, weekday-weekend differences were most prominent between 09:00 h and 19:00 h. In particular, the residential (HDB and RES) weekend values were higher during this period, but did not show the traffic-related weekday morning rush hour peak.

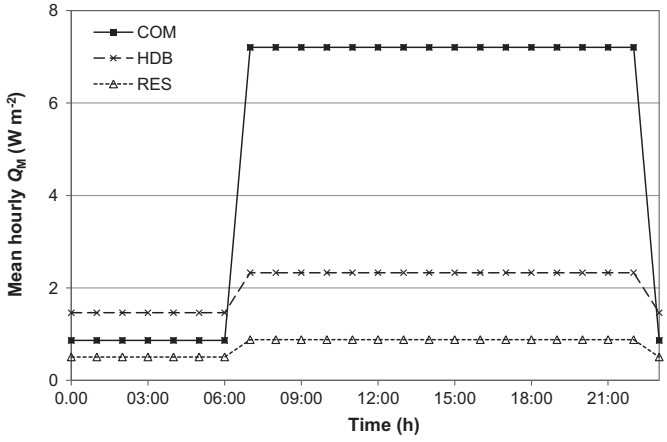

Fig. 5. Same as Fig. 3 but for Q_M.

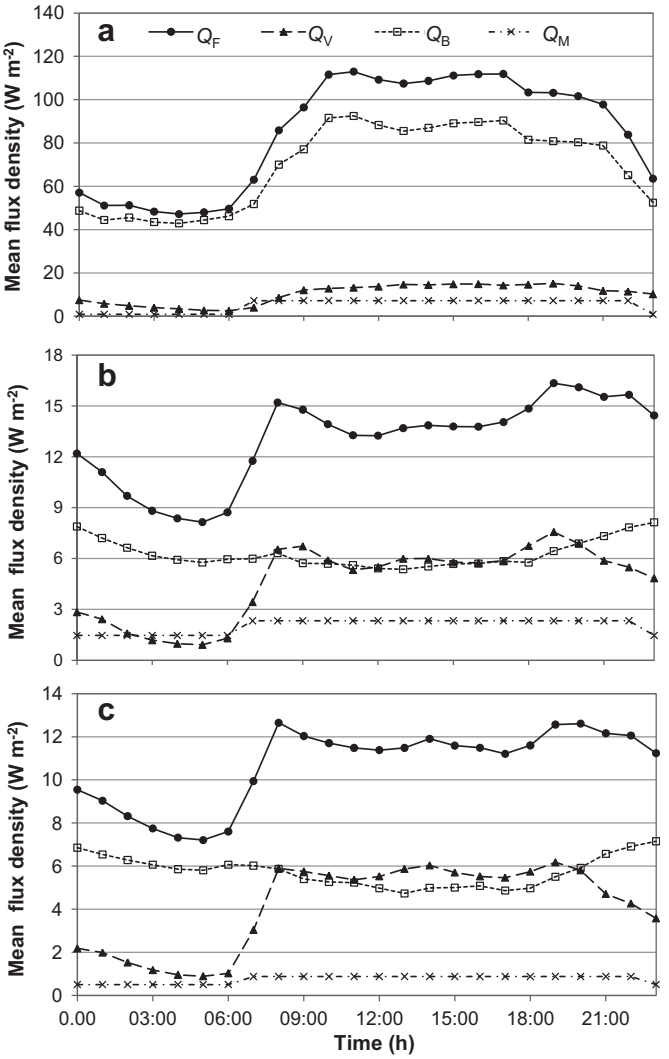

Fig. 6. Ensemble average from 181 days of diurnal variation of Q_F, Q_V, Q_B and Q_M for (a) COM, (b) HDB and (c) RES.

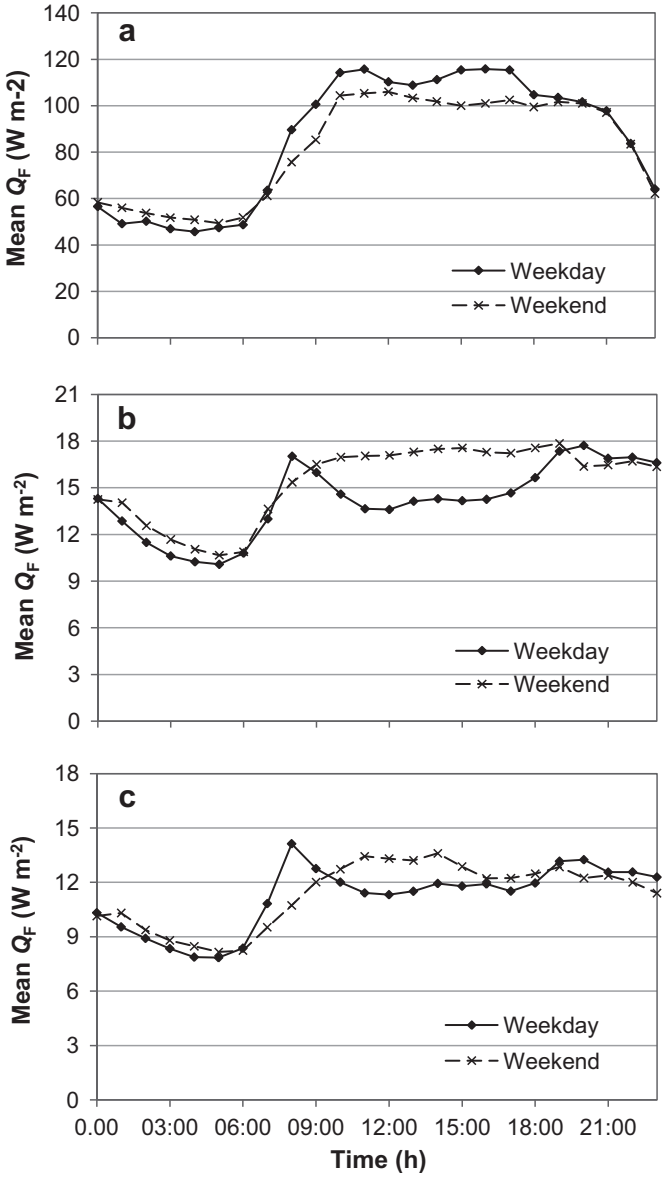

Fig. 7. Ensemble average from 181 days of diurnal variation of weekday and weekend Q_F values for (a) COM, (b) HDB and (c) RES.

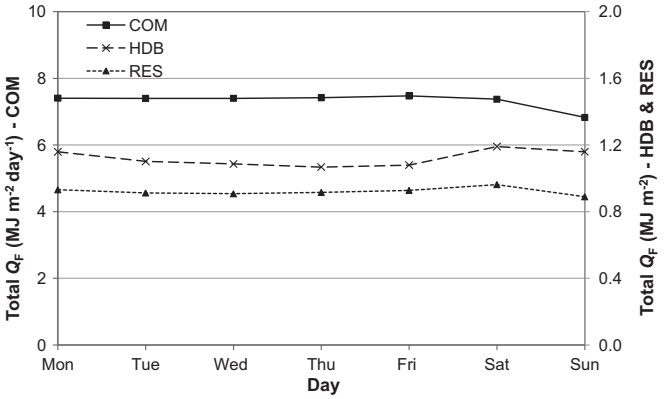

Fig. 8. Ensemble average from 6 months of weekly variation of Q_F for (a) COM and (b) HDB and RES.

Mean daily total Q_F values show relatively little variation across individual weekdays (Fig. 8). The maximum value is found in COM (7.5 MJ m^{-2} day^{-1}) on Friday, but even the lowest value on Sunday is only 10% smaller (6.8 MJ m^{-2} day^{-1}). The residential areas experienced peak values of 1.2 MJ m^{-2} day^{-1} (HDB) and 1.0 MJ m^{-2} day^{-1} (RES) on Saturday and minimum values on Sunday at RES (0.9 MJ m^{-2} day^{-1}) and Thursday at HDB (1.1 MJ m^{-2} day^{-1}). Variation of weekday mean daily total Q_F and the weekday-weekend differences were less than 10% for all three study areas.

The percentage breakdown for all components contributing to total Q_F is illustrated in Fig. 9. Building-related energy use was the dominant component of anthropogenic heat in each study area, contributing to Q_F at fairly similar proportions on weekdays (49–82%) and weekends (46–81%). Heat emissions from vehicles in the residential areas of HDB and RES contributed to just over a third of Q_F on weekdays and weekends whereas at COM, Q_V contributed to a smaller proportion (12% on weekdays and weekends) for every day of the week. Metabolic heat release formed the smallest component of Q_F in each of the three study areas on both weekdays and weekends. At COM and RES, Q_M accounted for less than 10% of Q_F throughout the week. However, the high-density housing area of HDB saw Q_M contributing to a relatively higher proportion (13% on weekdays; 21% on weekends).

5. Discussion

5.1. Temporal variability of Q_F estimates

Given that the present study includes some of the first detailed results of anthropogenic heat emissions in a tropical city, it is useful to compare the results to similar work carried out in cites located in other climatic regions. Of particular interest are building-related emissions which usually contribute most to Q_F, but very much depend on heating or cooling needs which are primarily determined by climate or seasonal temperature characteristics. Table 6 summarises results obtained for various city centres/commercial areas where appropriate numbers are available. The present magnitudes for COM are similar to summer values estimated for commercial areas in Tokyo (Ginza and Shinjuku) and winter values in Toulouse. This result can be explained by the fact that summers in Tokyo are very similar to the general climate in Singapore when even nighttime temperatures do not typically fall below 23 °C, i.e. necessitating the use of air-conditioning during most hours of the day. The large winter values in Toulouse on the other hand are due to space heating needs given the cool climate. The diurnal

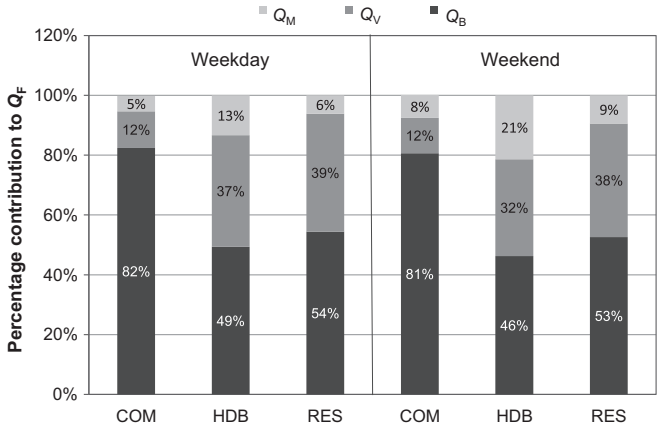

Fig. 9. Percentage breakdown of the individual components contributing to Q_F for COM, HDB and RES on weekdays and weekends.

Table 6
Representative hourly Q_F magnitudes of various (a) city centres/commercial areas, and (b) suburban residential areas.

Year	City[a]	Q_F (W m^{-2})			Source
		Annual	Summer	Winter	
(a) *City centres/commercial area*					
1986–94	Tokyo (Ginza)	–	86[b]	–	Moriwaki et al. (2008)
1986–94	Tokyo (Shinjuku)	–	136[b]	–	Moriwaki et al. (2008)
2001–02	Basel	20	–	–	Christen and Vogt (2004)
2004–05	Toulouse	–	25	100	Pigeon et al. (2007)
2008	Greater Manchester (various centres)	23	–	–	Smith et al. (2009)
2008–09	Singapore (COM)	85[c]	–	–	Present study
(b) *Suburban residential areas*					
1986–94	Tokyo (Kugahara)	–	18[b]	–	Moriwaki et al. (2008)
1987	Vancouver	–	–	~11	Grimmond (1992)
2001–02	Basel	5	–	–	Christen and Vogt (2004)
2004–05	Toulouse	–	<5	5–25	Pigeon et al. (2007)
2008–09	Singapore (HDB)	13[c]	–	–	Present study
2008–09	Singapore (RES)	11[c]	–	–	Present study

[a] Specific commercial area/city centre indicated in parenthesis.
[b] Represents mean hourly value at 14:00 h.
[c] Represents mean hourly value. For comparisons with Tokyo values, mean hourly values at 14:00 h are 109 W m^{-2} (COM), 16 W m^{-2} (HDB) and 13 W m^{-2} (RES).

variability of Q_F for COM also shows similarities to the winter profile found in the commercial areas of Tokyo (Moriwaki et al., 2008). The annual total Q_F values for the city centres of Basel and the Greater Manchester region as well as the summer value for Toulouse are considerably smaller compared to values calculated for COM because they are either averages across seasons or for the summer in a temperate climate where there is little need for space cooling.

In the case of residential areas, daily average Q_F values for HDB and RES were similar to the winter values for suburban Vancouver and Toulouse (Table 6). This is probably because the energy consumed to meet the heating needs in the case of the two mid-latitude cities is comparable to the average amount of energy used for air-conditioning in Singapore's residential areas. There is again good correspondence with the summer values from Tokyo, which are primarily accounted for by energy used for space cooling in both cities. The annual Q_F value for Basel and summer value for Toulouse are as expected lower than calculated for the residential areas in Singapore.

5.2. Comparison of Q_F against net all-wave radiation flux density

In order to obtain an indication of the likely importance of anthropogenic heat emissions relative to the net energy input into the urban system across the common land use types in Singapore, the mean diurnal Q_F values were compared with measurements of Q^* which were available for RES and assumed to be similar at COM and HDB. A net radiation surplus was observed between 08:00 h and 18:00 h, with mean hourly Q^* values reaching a maximum of 454 W m^{-2} at 13:00 h (~12:00 h solar time) (Fig. 10). For this period, magnitudes of mean Q_F were ~40% (COM), 5% (HDB) and 4% (RES) of Q^* values. Between 19:00 h and 07:00 h net radiation was about −50 W m^{-2} whereas Q_F values were ~143% (COM), 26% (HDB) and 21% (RES) of Q^*, but positive. When averaged over the entire day, Q_F was equivalent to 87% (7.3 MJ m^{-2} day^{-1}) of Q^* at COM. The relatively equal importance of Q^* and Q_F on a daily scale results primarily from the strong demands for air-conditioning by the energy intensive buildings located in the commercial area (Fig. 6). At HDB and RES, Q_F was equivalent to about 13% (1.1 MJ m^{-2} day^{-1}) and 11% (0.9 MJ m^{-2} day^{-1}) of Q^*, respectively. Similarly, Grimmond (1992) estimated that Q_F contributed more than 10% to the winter energy balance of suburban Vancouver. Although the contributions of Q_F to the energy balance of HDB and RES are comparatively lower than at COM, they cannot be ignored in the UEB (Eq. (1)) of suburban and much less so in the case of commercial areas.

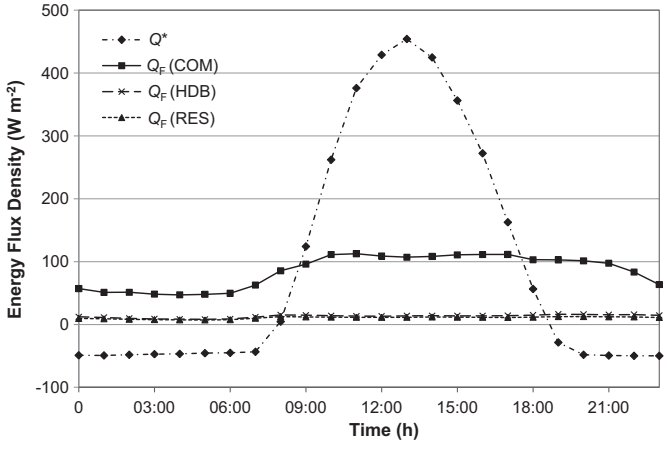

Fig. 10. Mean hourly net all-wave radiation flux density at RES (average from 2006 to 2008) and anthropogenic heat flux density profiles for all 3 study areas.

6. Summary and conclusions

The present paper provides one of the first detailed assessments of Q_F for a tropical city. Specifically, the diurnal and weekly variability of the anthropogenic heat flux density has been estimated for three land use types in Singapore (COM – commercial; HDB – high-density public housing; and RES – low-density residential) using the inventory-based modelling approaches of energy consumption for the period October 2008 to March 2009. The main findings obtained from the present study are:

(i) The largest mean hourly Q_F estimates of 113 W m^{-2} were found in COM at ~11:00 h. Maximum mean hourly Q_F values were substantially lower at the two residential study sites, HDB (17 W m^{-2}) and RES (13 W m^{-2}) at ~19:00–20:00 h, respectively.
(ii) Weekday mean hourly Q_F values for COM were on average about 5% higher than weekend values. At HDB and RES, the reverse was observed and average weekday values were approximately 9% (HDB) and 2% (RES) lower than their respective weekend estimates.

(iii) A distinct diurnal and weekly variability in the Q_F estimates was observed. Mean hourly Q_F at COM remained relatively large during the period of commercial activity (08:00–22:00 h) and became smaller when commercial activity ceased. Dual peaks that were observed in the mean hourly Q_F profiles of HDB and RES correspond to morning and evening rush hours. In terms of weekly variability, the daily total Q_F values for COM were higher on weekdays than on weekends, whereas the reverse was observed for HDB and RES. These diurnal and weekly variations of Q_F can be explained by variability in commuting patterns over the course of a day/week.

(iv) Buildings were the dominant contributor to anthropogenic heat in each study area, making up 83% (COM), 54% (RES) and 49% (HDB) of the respective weekday mean hourly Q_F estimates, and with very similar numbers for weekends. Throughout the week, Q_V accounted for just over a third of the mean hourly Q_F values for HDB and RES. the relative importance of Q_V at COM is smaller (12%) on both weekdays and weekends. Q_M was consistently the least important component of Q_F, making up 5–9% of anthropogenic heat emissions at COM and RES, and 13–21% at HDB over the course of a week.

(v) During daytime mean Q_F as a fraction of the net radiation input into the system is largest for COM (40%) and below 5% for the residential areas. Nighttime percentages are higher and in the case of COM ~143% of Q_F, but of opposite sign. Average daily Q_F is equivalent to 87% of Q^* at COM and considerably smaller at the two residential sites where Q_F is equivalent to 13% (HDB) and 11% (RES) of Q^*, respectively.

Many studies frequently mention that Q_F is largest in mid-latitude cities during winter due to demands for heating (e.g. Grimmond, 1992; Klysik, 1996; Sailor and Lu, 2004; Pigeon et al., 2007). However, the present research shows that Q_F can also be substantial in hot, tropical cities owing to strong demands for air-conditioning. Unlike in mid-latitude cities where Q_F exhibits clear seasonal variability, Q_F in tropical cities can remain high throughout the year and be of the same order of magnitude as calculated for city centres in mid-latitude cities during winter time.

The present study also showed that Q_F is an important component of the UEB in the commercial district, with nighttime values that are of similar magnitude to those of net radiation. Several implications follow from this result in terms of UHI research, UHI mitigation and more sustainable city design. Local UHI studies usually find the largest nocturnal heat island intensities in the vicinity of Orchard Road which is part of COM, whereas other areas with even higher building density and less vegetation, such as the financial district, have lower UHI magnitudes (Chow and Roth, 2006). Besides other possible influences particular to the local context, it is reasonable to assume that the large UHI magnitudes observed in the commercial district are also due to the additional Q_F contribution which is of lesser importance in the financial district which experiences reduced commercial activity in the evening.

A number of past studies have already noted the particular role Q_F can play in the genesis of the heat UHI. Contributions from Q_F have for example been used to explain the early evening UHI peak observed in Mexico City (Jauregui, 1997) or the large UHI intensities in Lodz during winter (Klysik and Fortuniak, 1999) when the incoming shortwave radiation is weak and heating demand strong. Other studies addressing this issue include Kimura and Takahashi (1991) and Kondo and Kikegawa (2003). Several studies have also tried to model the impact of Q_F on the UHI. Temperature simulations by Fan and Sailor (2005) showed that during the winter months Q_F (estimated to be 90 W m^{-2}) contributed about 2–3 °C to the nighttime heat island in Philadelphia. In mid-latitude cities, the impact of Q_F on the UHI is likely to be the largest within the city core during winter when heating demand is strong (e.g. Ichinose et al., 1999; Fan and Sailor, 2005). As shown in the present study, densely built and developed tropical cities are also likely to experience significant levels of Q_F in their commercial centres due to high energy demands for building air-conditioning. Such large anthropogenic heat emissions are not only likely to contribute to the UHI effect, but also represent an urban energy budget term that cannot be ignored. Such large Q_F values warrant further investigation to be able to fully judge their relevance for urban climates.

Acknowledgements

The authors are grateful for the financial support received from the National University of Singapore (Academic Research Fund) under grant R-109-000-091-112 for this study. The Land Transport Authority, Energy Market Authority and Housing and Development Board have supplied important secondary data.

References

Bach, W., 1970. An urban circulation model. Archives for Meteorology. Geophysics and Bioclimatology Series B 18, 155–168.
Bornstein, R.D., 1968. Observations of the urban heat island effect in New York City. Journal of Applied Meteorology 7, 575–582.
Chen, Y., Jiang, W.M., Zhang, N., He, X.F., Zhou, R.W., 2009. Numerical simulation of the anthropogenic heat effect on urban boundary layer structure. Theoretical and Applied Climatology 97, 123–134.
Chow, W.T.L., Roth, M., 2006. Temporal dynamics of the heat island of Singapore. International Journal of Climatology 26, 2243–2260.
Christen, A., Vogt, R., 2004. Energy and radiation balance of a central European city. International Journal of Climatology 24, 1395–1421.
Department of Health, Education and Welfare, 1967. New Jersey Air Pollution Activity Technical Report. United States Department of Health, Education and Welfare, Washington D.C.
Fan, H., Sailor, D.J., 2005. Modeling the impacts of anthropogenic heating on the urban climate of Philadelphia: a comparison of implementations in two PBL schemes. Atmospheric Environment 39 (1), 73–84.
Fanger, P.O., 1972. Thermal Comfort: Analysis and Applications in Environmental Engineering. McGraw-Hill, New York.
Ferreira, M.J., de Oliveira, A.P., Soares, J., 2011. Anthropogenic heat in the city of São Paulo, Brazil. Theoretical and Applied Climatology 104, 43–56.
Garcia-Cueto, R., Jauregui, E., Tejeda, A., 2003. Urban/rural energy balance observations in a desert city in northern Mexico. In: Paper Presented at the 5th International Conference on Urban Climate, Lodz, Poland.
Garnett, A., Bach, W., 1965. An estimation of the ratio of artificial heat generation to natural radiation heat in Sheffield. Monthly Weather Review 93, 383–385.
Grimmond, C.B.S., 1992. The suburban energy balance: methodological considerations and results for a mid-latitude west coast city under winter and spring conditions. International Journal of Climatology 12, 481–497.
Grimmond, C.B.S., Oke, T.R., 1999. Heat storage in urban areas: local scale observations and evaluation of a simple model. Journal of Applied Meteorology 38, 922–940.
Harleman, D.R.F., 1971. Heat, the Ultimate Waste. Technology Review December 1971, pp. 44–51.
Ichinose, T., Shimodozono, K., Hanaki, K., 1999. Impact of anthropogenic heat on urban climate in Tokyo. Atmospheric Environment 33, 3897–3909.
International Energy Agency, 2008a. World Energy Outlook 2008. International Energy Agency, Paris.
International Energy Agency, 2008b. 2006 Energy Balance for Singapore. http://www.iea.org/stats/balancetable.asp%3fCOUNTRY_CODE=SG.
International Energy Agency, 2009. World Energy Outlook 2009. International Energy Agency, Paris.
Jauregui, E., 1997. Heat island development in Mexico City. Atmospheric Environment 31 (2), 3821–3831.
Kalma, J.D., Aston, A.R., Millington, R.J., 1972. Energy use in the Sydney area. Proceedings of the Ecological Society of Australia 7, 125–142.
Kalma, J.D., Byrne, G.F., 1975. Energy use and the urban environment: some implications for planning. In: Proceedings of the Symposium on Meteorology Related to Urban and Regional Land Use Planning. World Meteorological Organisation, Geneva, pp. 237–258.
Kimura, F., Takahashi, S., 1991. The effects of land-use and anthropogenic heating on the surface temperature in the Tokyo metropolitan area: a numerical experiment. Atmospheric Environment 25B (2), 155–164.
Klysik, K., 1996. Spatial and seasonal distribution of anthropogenic heat emissions in Lodz, Poland. Atmospheric Environment 30 (20), 3397–3404.
Klysik, K., Fortuniak, K., 1999. Temporal and spatial characteristics of the urban heat island of Lodz, Poland. Atmospheric Environment 33, 3885–3895.
Kondo, H., Kikegawa, Y., 2003. Temperature variation in the urban canopy with anthropogenic energy use. Pure and Applied Geophysics 160, 317–324.

Land Transport Authority, 2008. Annual Vehicle Statistics 2008 URL: http://www.lta.gov.sg/corp_info/doc/MVP01-4%2520(MVP%2520by%2520fuel).pdf.
Lee, S.H., Song, C.K., Baik, J.J., Park, S.U., 2009. Estimation of anthropogenic heat emission in the Gyeong-In region of Korea. Theoretical and Applied Climatology 96 (3–4), 291–303.
Ministry of Education, 2002. Ministry of Education Headquarters Building Energy Audit Report. Ministry of Education, Singapore.
Ministry of the Environment and Water Resources, 2009. A Lively and Liveable Singapore: Strategies for Sustainable Growth. Ministry of Environment and Water Resources, Singapore.
Moriwaki, R., Kanda, M., Senoo, H., Hagishima, A., Kinouchi, T., 2008. Anthropogenic water vapor emissions in Tokyo. Water Resources Research 44, W11424.
National Environment Agency, 2009. Weatherwise. National Environment Agency, Singapore.
National Institute of Education, 2003. National Institute of Education Energy Audit Report. National Institute of Education, Singapore.
Newcombe, K., 1976. Energy use in Hong Kong: part III, spatial and temporal patterns'. Urban Ecology 2, 139–172.
Offerle, B., Jonsson, P., Eliasson, I., Grimmond, C.S.B., 2005. Urban modification of the surface energy balance in the West African Sahel: Ouagadougou, Burkina Faso. Journal of Climate 18, 3983–3995.
Oke, T.R., 1987. Boundary Layer Climates, second ed. Methuen, London.
Oke, T.R., 1988. The urban energy balance. Progress in Physical Geography 12, 471–508.
Ojima, T., Moriyama, M., 1982. Earth surface balance changes caused by urbanisation. Energy and Buildings 4, 99–114.
Pigeon, G., Legain, D., Durand, P., Masson, V., 2007. Anthropogenic heat release in an old European agglomeration (Toulouse, France). International Journal of Climatology 27, 1969–1981.
Plaza Singapura, 2006. Plaza Singapura Energy Audit Report. Plaza Singapura, Singapore.
PREMAS Energy Centre, 2004. Energy Audit of Selected HDB Residential Blocks in Singapore. PREMAS International, Singapore.
Probald, F., 1972. Deviations in the heat balance: the basis of Budapest's urban climate. In: Adams, W.P., Helleiner, I.M. (Eds.), International Geography 1972. University of Toronto Press, Toronto, pp. 184–186.
Roth, M., 2007. Review of urban climate research in (sub)tropical regions. International Journal of Climatology 27, 1859–1873.
Sailor, D.J., 2011. A review of methods for estimating anthropogenic heat and moisture emissions in the urban environment. International Journal of Climatology 31 (2), 189–199.
Sailor, D.J., Lu, L., 2004. A top-down methodology for developing diurnal and seasonal anthropogenic heating profiles for urban areas. Atmospheric Environment 38, 2737–2748.
Shangri-la Hotel Singapore, 2002. Shangri-la Hotel (Singapore) Energy Audit Report. Shangri-la Hotel, Singapore.
SMIC, 1971. Inadvertent Climate Modification: Report of the Study on Man's Impact on Climate. Massachusetts Institute of Technology Press, Cambridge, Massachusetts.
Smith, C., Lindley, S., Levermore, G., 2009. Estimating spatial and temporal patterns of urban anthropogenic heat fluxes for UK cities: the case of Manchester. Theoretical and Applied Climatology 98, 19–35.
Spronken-Smith, R.A., 2002. Comparison of summer- and winter-time suburban energy fluxes in Christchurch, New Zealand. International Journal of Climatology 22, 979–992.
Spronken-Smith, R.A., Kossmann, M., Zawar-Reza, P., 2006. Where does all the energy go? Surface energy partitioning in suburban Christchurch under stable wintertime conditions. Theoretical and Applied Climatology 84, 137–149.
Steinecke, K., 1999. Urban climatological studies in the Reykjavik subarctic environment, Iceland. Atmospheric Environment 33, 4157–4162.
Swaid, H., 1993. Urban climate effects of artificial heat sources and ground shadowing by buildings. International Journal of Climatology 13, 797–812.
Taha, H., 1997. Urban climates and heat islands: albedo, evapotranspiration, and anthropogenic heat. Energy and Buildings 25, 99–103.
Tan Tock Seng Hospital, 2004. Tan Tock Seng Hospital Energy Audit Report. Tan Tock Seng Hospital, Singapore.
Tejeda, A., Jauregui, E., 2005. Surface energy balance measurements in the Mexico City region: a review. Atmosfera 18, 1–23.
The American Club Singapore, 2004. The American Club Singapore Energy Audit Report. The American Club Singapore, Singapore.
Thong, M.T.L., Ho, M.H.C., Sim, S.P., 2005. Energy conservation measures for rapid transit system in Singapore. In: Paper Presented at the 7th International Conference on Power Engineering Singapore.
Torrance, K.E., Shum, J.S.W., 1976. Time-varying energy consumption as a factor in urban climate. Atmospheric Environment 10, 329–337.
Urban and Redevelopment Authority, 2008. Master Plan 2008 URL: http://www.ura.gov.sg/mp08/map.jsf%3fgoToRegion=SIN.
Volkswagen, 2008. Volkswagen Commercial Vehicles URL: http://www.vwasia.com/publish/vwasia/singapore/en/commercial_vehicles.html.
Yap, D., Oke, T.R., 1974. Sensible heat fluxes over an urban area: Vancouver. Archives for Meteorology, Geophysics and Bioclimatology, Series B 23, 69–80.